Mitigating Blurring Artifacts in 3D Snapshot CEST MRI through Tailored Flip Angle Train Optimization

Simon Weinmüller[1], Jonathan Endres[1], Moritz Zaiss[1,2]

[1] *Institute of Neuroradiology, University Clinic Erlangen, Friedrich-Alexander-Universität Erlangen-Nürnberg, Erlangen, Germany*

[2] *Department Artificial Intelligence in Biomedical Engineering, Friedrich-Alexander Universität Erlangen-Nürnberg, Erlangen, Germany*

INTRODUCTION In Chemical Exchange Saturation Transfer (CEST) MRI measurements, one challenge is to measure prepared longitudinal magnetization fast and precisely. However, the readout itself alters the prepared magnetization during acquisition, leading to blurring effects. In the spiral-centric-reordered 3D GRE snapshot [1], the prepared magnetization decays towards the steady state with the T1-Look-Locker-decay rate leading to blurring that affects image intensity, quality and contrast. To reduce this effect, we optimized a sequence with variable flip angle (vFA) using the MR-zero framework [2] with a fully differentiable Phase Distribution Graph [3] simulation to achieve a better estimation of the prepared magnetization.

METHODS To simplify the optimization problem, an inversion recovery sequence (TI=3s) was used as CEST surrogate during the training. The image loss was calculated based on the magnitude of the normalized magnetization prepared image. The GRE Snapshot sequence parameters are the following: matrix: 96x96x4, FOV: 200x200x20 mm^3, TE: 3.2ms, TR: 5.1ms, spiral elongation factor: 0.5, bandwidth: 500Hz/pixel. For comparison of the vFA sequence, a constant flip angle of 5° (cFA 5°) was used for 384 repetitions.
The target of the optimization process is a fully segmented image, where every k-space line is prepared individually. For measurement close to ideal state, an 8-shot sequence was used due to measured time vs. sharpness compromise.
The tailored vFA train was subsequently combined with the low power multi-pool CEST protocol [4,5], with saturation at B1rms=0.9 µT at 56 different frequency offsets.
Signal simulations and optimization were performed using the Phase Distribution Graph algorithm [2,3], using brain data generated from the BrainWeb [6] database.
Two healthy subjects were scanned after written informed consent and under approval of the local ethics committee, at a MAGNETOM Prisma 3T scanner (Siemens Healthcare GmbH, Erlangen, Germany).

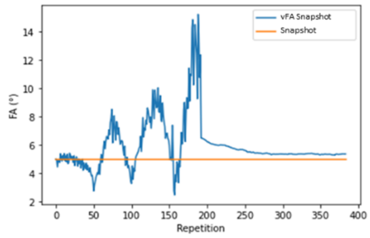

Fig. 1: Constant and tailored flip angle train. Structures emerge due to LL-decay and 3D reordering.

RESULTS The vFA pattern is shown in Figure 1. With varying the flip angles the measurement of a prepared magnetization can be improved as shown exemplary for one slice in Figure 2. Sharper images, a lower RMSE and higher SSIM can be achieved using vFA. The difference images to the measured 8-shot sequence show a clear reduction of relaxation effects. This also translates to the CEST measurement where better contrast is achieved and finer structures are resolved (red arrows, Figure 3). The profile plot in Figure 3g reveals especially shaper and darker minima, an indication for reduced image blurring.

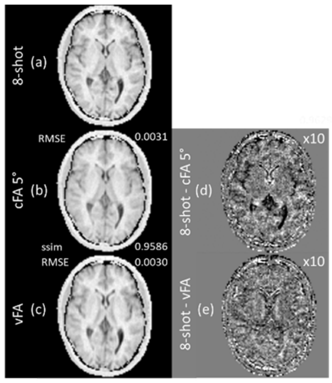

Fig. 2: (a) 8-shot snapshot; (b) snapshot with constant FA of 5°; (c) vFA snapshot, difference image (d, e).

DISCUSSION & CONCLUSION Here, we demonstrated the removal of T1 Look-Locker-blurring by a flip angle optimization for a 3D GRE snapshot sequence as commonly used for CEST MRI. Compared to previous published flip angle shapes [7], we found new k-space-reordering-tailored patterns reducing image blurring. This potentially allows us to further increase flip angle and number of slices for higher signal and more coverage within one snapshot CEST readout. An improved visibility of CEST features is especially important for fast high-resolution CEST in pathologies.

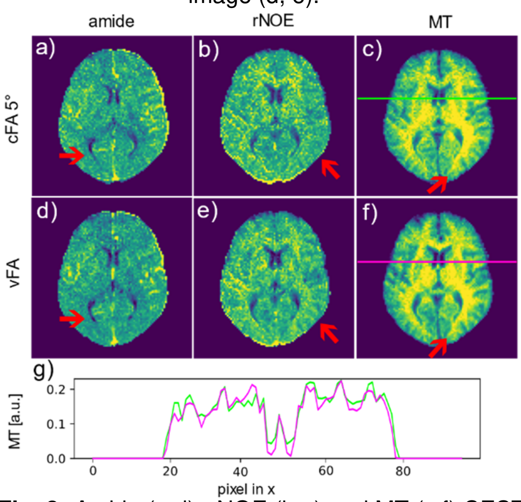

Fig. 3: Amide (a,d), rNOE (b,e) and MT (c,f) CEST maps for cFA 5° and vFA. Profile plot (g) of MT image intensity along lines defined in c) and f)

REFERENCES

1. Zaiss M, *et al.* NBM 2018. doi: 10.1002/nbm.3879
2. Loktyshin A, *et al.* MRM 2021. doi: https://doi.org/10.1002/mrm.28727
3. Endres J, *et al.* MRM 2024. doi: 10.1002/mrm.30055
4. Glang F, *et al.* MRM 2020. doi: 10.1002/mrm.28117
5. Pulseq-CEST. https://github.com/kherz/pulseq-cest-library/tree/master/seq-library/MultiPool_3T_002_0p9uT_80Gauss_DC50_3200ms_deepCEST
6. BrainWeb: Simulated Brain Database. Accessed January 1, 2023. https://brainweb.bic.mni.mcgill.ca/brainweb/
7. Stehling M, *et al.* MRI 1992. doi: https://doi.org/10.1016/0730-725X(92)90387-F